THE CASE FOR A ZERO-NOISE CCD ON A HIGH-RESOLUTION OPTICAL SPECTROGRAPH

Étienne Artigau[1], Olivier Daigle[2,1], René Doyon[1], Claude Carignan[1]

ABSTRACT

We present the case for using a zero-noise CCD as the science array in a high-resolution optical spectrograph (HROS). The Université de Montréal Laboratoire d'Astrophysique Expérimentale instrumentation group in collaboration with the Laboratoire d'Astrophysique de Marseille has developed zero readout noise CCDs. The first generation of small devices (512 x 512 arrays) were used for low-flux Fabry-Perot observations of galaxies, but the development of large format (4K x 4K) zero-noise arrays makes them appealing for a broader suite of instruments. We argue that using a zero-noise CCD would significantly increase the capabilities of a HROS to observe faint targets. On faint targets, existing HROS are limited by readout noise between telluric OH lines and one generally looses significantly by binning spectrally compared to a classical low-resolution spectrograph. By using zero-noise CCDs on a HROS one can mask OH lines in post-processing and arbitrarily degrade the resolution, allowing the study of very faint objects at moderate ($R \sim 100 - 1000$) resolution. Such an instrument would be only limited by the continuum night sky emission, providing a three-fold gain in efficiency over the far-red domain. The gain is not only in terms of efficiency, but also allows one to select a posteriori the effective resolution without loss. This is ideal for the observation of rapid transients such as those that will be found by LSST. The arrays described here also open a niche, currently empty in the Gemini instrument suite, for high time-resolution ($> 1 \, \mathrm{Hz}$) spectroscopic observations. We stress that zero-noise CCDs also feature a "classical" output for very high fluxes or observations not limited by readout noise.

Subject headings:

1. INTRODUCTION

This white paper makes a case for using a photon-counting device as a science detector for a high-resolution optical spectrograph (HROS). It does not make, in itself, a science case for any specific project to be undertaken with a HROS at Gemini, but intends to highlight a major science niche that can be opened with such an instrument by using *demonstrated* innovative detector technologies.

2. STRAW-MAN SPECTROGRAPH AND DETECTOR FORMAT

To quantify the benefits of this approach, we opted to define a straw-man spectrograph with characteristics we felt were reasonable for a HROS at Gemini. All calculations performed later assume that the instrument has the characteristics listed in Table 1.

It is important for the instrumental discussion to determine the detector format required to meet the science goals of the proposed HROS. Assuming the straw-man spectrograph described above and a 3 pixel sampling, one requires about ∼120 000 spectral pixels. Assuming 40 orders on the detector, the orders will be ∼3000 pixels long. A square formatting (i.e. 3000 pixels in the cross-dispersion direction) leaves 3000/40∼ 75 pixel per order on average. Using a slit width of 0.3″ per pixel, the inter-order spacing would correspond to 22.5″. Obviously inter-order spacing is wavelength dependent and it is desirable to leave a few intra-orders pixels without illumination implying that slit lengths up to 10 − 15″ are

Electronic address: artigau@astro.umontreal.ca; odaigle@astro.umontreal.ca; doyon@astro.umontreal.ca; claude@astro.umontreal.ca

[1] Département de Physique and Observatoire du Mont Mégantic, Université de Montréal, C.P. 6128, Succ. Centre-Ville, Montréal, QC, H3C 3J7, Canada

[2] Nuvu Camera

TABLE 1
STRAW-MAN SPECTROGRAPH

Resolution	$R = 40000$
Spectral coverage	$400 - 1000 \, \mathrm{nm}$
Slit size	$0.8'' \times 10''$
Effective aperture[a]	$0.8'' \times 0.8''$
Global transmission	25%
Primary size	$8.1 \, \mathrm{m}$
Readout noise, classical CCD	$3 \, \mathrm{e}^-$
Readout noise, photon counting [b]	$1 \times 10^{-3} \mathrm{e}^-$
Pixel per resolution element [c]	10
Continuum sky emission [d]	$7 \times 10^{-17} \mathrm{erg/s/cm^2/Å}$

[a]Size of the extraction box in the broad sense. Could be the effective fiber size on sky or a slit width times the width of the extraction box along the spectrum trace.

[b]Readout noises below 1 e⁻ clearly do NOT follow Gaussian statistics. This is an equivalent noise, corresponding to 1 clock-induced charge per 1000 pixel per readout.

[c]We assume that the resolution element spawns 3.2 pixel in the spectral dimension and 3.2 pixel in the spatial dimension. With a fiber-fed spectrograph this would correspond to the dimension perpendicular to dispersion, not a true spatial dimension. This sampling is likely to be close but above Nyquist sampling.

[d]The high resolution spectrum used for all computations detailed here can be obtained at the following address : http://www.eso.org/observing/dfo/quality/UVES/pipeline /sky_spectrum.html

probably realistic. This provides a significant 1-D spatial resolution, ∼20 FWHM under good seeing conditions, that can be interesting for studies of small, spatially extended objects. A 3K x 3K detector would be sufficient to meet the straw-man spectrograph design but we assumed here a 4K x 4K detector to leave some margin for a longer slit, a higher resolution or a finer sampling.

3. EMCCD DEVELOPMENT AT THE LAE

The Laboratoire d'Astrophysique Expérimentale (LAE) has been doing work on photon counting cameras for the last 10 years. This work was done in close partnership with the Laboratoire d'Astrophysique de Marseille (LAM). The first such camera, called FaNTOmM (Gach et al. 2002; Hernandez et al. 2003), was based on a GaAs Hamamatsu amplifier tube in front of a DALSA CCD. Despite its Detective Quantum Efficiency (DQE) of only $\sim 25\%$, this camera with essentially zero read-out noise (RON) would, at very low light level, outperform a standard CCD with DQE 80% but with typical RON of $3\,e^-$. Another similar instrument, called GHaFaS (Carignan et al. 2008; Hernandez et al. 2008) was also built for the WHT.

The tube amplifier technology was gradually replaced in the last five years by Electron Multiplying CCDs (EM-CCDs) due to their higher quantum efficiency and relative ease of use. The first tests with EMCCD were done with a commercially available camera from ANDOR. We first tried to build a controller that could reproduce those results (Daigle et al. 2004). It became rapidly clear that the limiting factor to be able to do photon counting was the level of the Clock Induced Charge (CIC) noise (Daigle et al. 2006b). Recently (Daigle et al. 2008), a new controller, the CCD Controller for Counting Photons (CCCP), was built that could reduce the CIC by more than a factor of 10 compared to what had been done before. Tests on the sky showed that the same signal to noise ratio could be achieved 5 times faster with the CCCP system than with the FaNTOmM camera. Up to now, zero-noise imagers developed at the LAE were used for integral-field spectroscopy (Fabry-Perot, $R \sim 15\,000$) of galaxies and H_{II} regions for kinematic measurements (Daigle et al. 2006a; Chemin et al. 2006; Dicaire et al. 2008), galactic dynamics (Hernandez et al. 2005; Fathi et al. 2008) and galaxy evolution (Shapiro et al. 2008).

CCCP was used so far with existing 512×512 (CCD97) at the Observatoire du Mont Mégantic (Daigle et al. 2009). The LAE just obtained a Canadian Fund for Innovation (CFI) grant to develop a larger EMCCD detector with $e2v$, hopefully a $4K \times 4K$ ($4K \times 8K$ for frame transfer (FT) chips). It should be straightforward to extend the capabilities of CCCP to those large chips which will take about 2 years to develop. Once this is done, they will allow building the ideal (high DQE and zero RON) large format ($4K \times 4K$) cameras.

Photon counting CCDs also have a classical output with a moderate ($\sim 3\ e^-$) readout noise. The photon counting mode may not provide a significant gain in certain types of observations and one may prefer to use the classical output in that case. This may be the case, for example, when observing very bright targets where systematics, rather than photon or readout noise, dominate the error budget.

4. OH SUPPRESSION WITH A HIGH-RESOLUTION SPECTROGRAPH

The sky background in the $0.6 - 1.0\,\mu m$ domain has two main contributions: a large number of very narrow emission lines due to the hydroxyl radical (OH) and a low-level continuum. At low resolution (i.e. $R <$5000), the OH lines blend into a forest of lines that dominate the sky contribution over most resolution elements. These OH lines affect sensitivity of low-resolution spectroscopy for two reasons: they vary in intensity over time-scales of a few minutes and contribute to the Poisson statistics in the object spectrum. The intrinsic time-variability of OH-lines impose an upper-limit on the delay between sky and object measurement (at most $1 - 2$ minutes) for very deep spectroscopy. This problem can be overcome by interleaving, within a single exposure, sky and object frames in what is now known as "nod-and-shuffle" mode.

Poisson noise from OH lines cannot be suppressed through rapid calibration of sky emission and can only be minimized by removing the flux from sky lines, either through optical or software suppression. One simple solution consists of dispersing the spectrum at a resolution significantly above that required to separate most OH lines ($R \sim 5000$), mask the OH lines by software and degrade the resolution by a simple binning. In practice, this technique cannot realistically be applied with existing spectrograph for a simple reason : readout noise. Even using low readout noise CCD ($\sim 3\,e^-$), the spectral binning effectively increases readout noise to levels that exceed the Poisson noise from the sky background continuum.

The ultimate source of background in the visible is the continuum sky emission. At high ecliptic latitude and under dark conditions, this background is at a level of $\sim 7 \times 10^{-17}\,\mathrm{erg/s/cm^2/\mathring{A}}$. Contrary to the OH line background, this continuum contribution is relatively constant over the whole optical to far-red domain ($400 - 1000\,\mathrm{nm}$). With the straw-man spectrograph described above, this corresponds to 0.1 photon per second per resolution element at $800\,\mathrm{nm}$ or 0.01 photon/s/pixel. For photon noise from the sky continuum to be the dominant source of noise (i.e. sky continuum noise $2\times$ larger than readout noise with a $3\,e^-$ RON), one will require 36 continuum photons/pixel or an integration time of about at least 1 hour. This would impose unrealistic constraints on observing sequences and render observing very inefficient for targets that require less than 1 hour of integration.

A high-resolution spectrograph with a CCD having a readout-noise significantly below $1\,e^-$ would open a new door to low-resolution spectroscopy. One could take a high-resolution spectrum of an object vastly too faint to be studied through high-resolution spectroscopy on existing telescopes, mask OH lines, degrade the spectral resolution through binning and extract a low-resolution spectrum with a sky-background limited only by the continuum contribution. The gain in observing, quantified in the following section, is a function of wavelength and binning, but at $R = 100$ binned resolution with the straw-man spectrograph, there is a mean gain between 700 and $1000\,\mathrm{nm}$ of ~ 3 relative to an $R = 100$ classical spectrograph. There are numerous science projects that would benefit from such a gain over that wavelength domain : high-z galaxy studies, brown dwarf spectroscopy, embedded objects, etc.

One added benefit that can hardly be quantified is that the final resolution can be determined *a posteriori*. For example, one could be interested in an $R = 100$ spectrum of a faint young brown dwarf to study broad molecular absorptions, but if upon analysis, the object shows prominent Hα emission, obtain a line profile at a resolution up to the spectrograph full resolution ($R = 40000$).
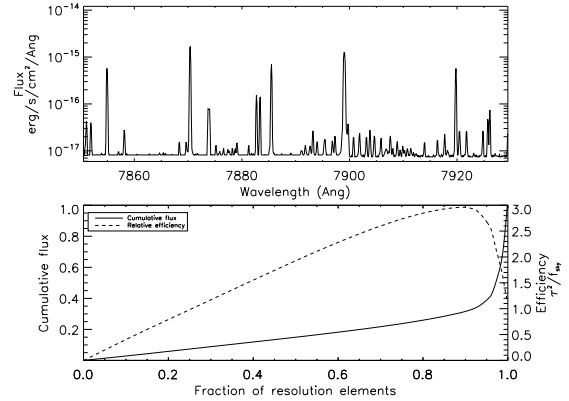
FIG. 1.— Top panel : sky spectrum at $R = 40000$ over a short far-red wavelength interval corresponding to a single $R = 100$ resolution element (same as in Figure 2 binning). The background is dominated by a large number of narrow emission lines that. A low-level background contributes to ~30% of the integrated background over that interval. Note the logarithmic scaling of the spectrum intensity. Bottom panel : Cumulative sky background flux; about 70% of the background comes from ~ 5 % of spectral resolution elements. Over that spectral interval, masking the ~ 15% brightest resolution elements would increase the observing efficiency three-fold.

TABLE 2
Continuum background for visible bands

band	λ	cont[c]	bgnd[d]	cont$c$ (80%)	bgnd[d] (80%)
	nm	mag	mag	mag	mag
g	468	21.5	21.3[a]	19.6	19.6[b]
r	616	21.2	20.9	20.2	20.1
i	748	21.3	20.4	20.6	20.1
z	893	21.1	19.6	20.8	19.5

All mags are in the Vega system
[a]Consistent with the 20%tile $V = 21.37$ reported on the Gemini website.
[b]Sky background is taken to be a Solar spectrum times a λ^{-4} Raleigh transmission adjusted in amplitude to get $g[Vega] = 19.61$.
[c]Continuum-only contribution to the sky background for dark and 80-percentile conditions
[d]Total sky background (line and continuum contributions) for dark and 80-percentile conditions

4.1. The arithmetics of background and observing efficiency

The signal-to-noise ratio (SN) of an observation can be estimated through the following relation :

$$SN = \frac{f_{target}t}{\sqrt{f_{target}t + f_{sky}t + r^2}},$$

where f_{sky} is the sky contribution (photon/s), f_{target} is the target contribution (photon/s), r is the readout noise (for multiple exposures, one would replace r^2 with $r_1^2 + r_2^2 + ... + r_n^2$) and t is the integration time (s).

In the regime where $f_{target}t \ll f_{sky}t$ and $r^2 \ll f_{sky}t$:

$$SN = \sqrt{t}\frac{f_{target}}{\sqrt{f_{sky}}}.$$

When adding a spectral mask to cut down sky emission, one needs to weigh the SN by the transmission (τ) of the mask. f_{sky} now corresponds to the sky background transmitted by the mask. The above equation now becomes :

$$SN = \sqrt{t}\frac{f_{target}\tau}{\sqrt{f_{sky}}}.$$

The time required to reach a given SN is :

$$t = SN^2\frac{(f_{target}\tau)^2}{f_{sky}}.$$

Assuming a fixed SN and f_{target}, the observing efficiency (η, proportional to the integration time required to reach a given SN for a given target) becomes :

$$\eta \propto \frac{\tau^2}{f_{sky}}.$$

One clearly wants to maximize η by keeping the background f_{sky} as low as possible for a spectral transmission as high as possible.

For this arithmetics to be true, it is important that the two conditions mentioned above be met. The flux density of the visible *continuum* contribution is relatively grey at 7×10^{-17} erg/s/cm²/Å .

5. A CAVEAT ON THE SKY VARIABILITY

Sky background is notoriously variable, even on Moonless nights. The continuum contribution comes from various sources such as zodiacal light, airglow, light pollution or diffused starlight and varies strongly as a function of ecliptic latitudes, season, etc. The line contribution of the sky spectrum is dominated by the OH molecule with a handful of lines (e.g. oxygen line at 557.7 nm) due to other chemical species. OH line emission dominates the near-infrared background up to $2.0\,\mu$m, where it shows a variability of up to 1 mag and a similar variability is expected in the OH-line emission over the optical domain. The values listed in Table 2 are consistent with typical conditions in dark sites; the spectrum used to derive these values were constructed from a set of very deep, dark time, exposures at Cerro Paranal and should constitute a realistic estimate of the Mauna Kea or Cerro Pachón night sky.

6. SCIENCE WITH A ZERO-NOISE CCD
6.1. Benefits at R=40000

The OH-suppression described earlier is not the only benefit of using a photon counting device. There are various benefits for spectroscopy at the nominal resolution of the spectrograph.

As pointed out in the case of low-resolution spectroscopy with OH suppression, the per-pixel limitation will be the continuum sky emission over most of the whole spectral domain, not readout noise. This will significantly increase the sensitivity even for targets that are significantly brighter than the night sky.

The very rapid frame rate allowed by the absence of readout noise allows a very large number of frames to be taken. Cosmic ray rejection is straightforward when one obtains a large number of short integrations. This will be especially important for faint targets, regardless of the desired resolution.

The rapid frame-rate implies that if observations are taken under very poor conditions, most likely in a band-4 program observing very bright targets, and that the
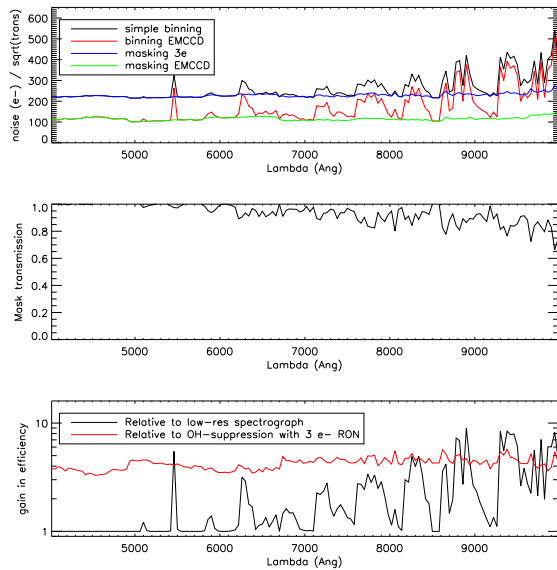
FIG. 2.— Top panel : noise for a binned spectra in the case of a background-limited source for 4 instrumental combinations. Simple binning of the straw-man spectrograph spectrum with a $3e^-$ RON, simple binning with a EMCCD, binning with OH-line masking and a $3e^-$ RON, binning and OH-line masking with an EMCCD. In all cases a final resolution of $R = 100$ and an exposure time of 1200 s. Middle panel : transmission of the OH-line mask. Bottom panel : gain in observing efficiency of the EMCCD OH-masking scheme compared to a R=100 spectrograph and a $3e^-$ straw-man spectrograph with OH-masking. Note that for nearly all resolution element, the $3e^-$ straw-man spectrograph is worse than a low-resolution spectrograph. This is why no current high-resolution spectrograph is routinely used for OH-suppression; the readout-noise cost overweights the gain in OH-line Poisson noise suppression.

sequence needs to be interrupted, the interruption will have little effect on the acquired science.

6.2. *Opening the time domain*

Also noteworthy, but beyond the scope of this white paper and certainly deserving a white paper in itself, is the interest for a high time-resolution (at least 1 Hz) HROS. A number of astrophysical objects vary on timescales shorter than the typical readout time of a large format CCD (tens of seconds), such as pulsars, flaring stars, accreting compact objects, etc. No current instrument at Gemini is capable of spectroscopy at such a frame rate, and a zero noise CCD could open this unique instrumental niche.

6.3. *Synergy with LSST*

The completion of the Large Synoptic Survey Telescope (LSST), the most highly ranked astronomical project in the US decadal survey, will certainly mark the second half of the upcoming decade. While in itself an unparalleled scientific tool, the LSST is likely to ultimately be limited by the follow-up capabilities of other astronomical observatories. Queue observing at Gemini certainly enables a very rapid response to transient events. One could wonder what would be the best instrument to observe a rapidly fading transient of unknown nature uncovered by a survey such as LSST. We argue that a HROS combined with a zero noise CCD would be the best instrument to characterize such a transient without knowing its nature. As pointed above, the resolution can be determined a posteriori allowing both high-resolution line profiles and broad spectroscopic features to be retrieved. OH suppression will allow one to push the sensitivity in the red for highly redshifted or embedded objects.

REFERENCES

Carignan, C., Hernandez, O., Gach, J., Balard, P., De Denus-Baillargeon, M., Fathi, K., Beckman, J., & Koulidiati, J. 2008, in Presented at the Society of Photo-Optical Instrumentation Engineers (SPIE) Conference, Vol. 7014, Society of Photo-Optical Instrumentation Engineers (SPIE) Conference Series

Chemin, L., Carignan, C., Drouin, N., & Freeman, K. C. 2006, AJ, 132, 2527

Daigle, O., Carignan, C., Amram, P., Hernandez, O., Chemin, L., Balkowski, C., & Kennicutt, R. 2006a, MNRAS, 367, 469

Daigle, O., Carignan, C., & Blais-Ouellette, S. 2006b, in Presented at the Society of Photo-Optical Instrumentation Engineers (SPIE) Conference, Vol. 6276, Society of Photo-Optical Instrumentation Engineers (SPIE) Conference Series

Daigle, O., Carignan, C., Gach, J., Guillaume, C., Lessard, S., Fortin, C., & Blais-Ouellette, S. 2009, PASP, 121, 866

Daigle, O., Gach, J., Guillaume, C., Carignan, C., Balard, P., & Boisin, O. 2004, in Presented at the Society of Photo-Optical Instrumentation Engineers (SPIE) Conference, Vol. 5499, Society of Photo-Optical Instrumentation Engineers (SPIE) Conference Series, ed. J. D. Garnett & J. W. Beletic, 219–227

Daigle, O., Gach, J., Guillaume, C., Lessard, S., Carignan, C., & Blais-Ouellette, S. 2008, in Presented at the Society of Photo-Optical Instrumentation Engineers (SPIE) Conference, Vol. 7014, Society of Photo-Optical Instrumentation Engineers (SPIE) Conference Series

Dicaire, I., Carignan, C., Amram, P., Marcelin, M., Hlavacek-Larrondo, J., de Denus-Baillargeon, M., Daigle, O., & Hernandez, O. 2008, AJ, 135, 2038

Fathi, K., Beckman, J. E., Lundgren, A. A., Carignan, C., Hernandez, O., Amram, P., Balard, P., Boulesteix, J., Gach, J., Knapen, J. H., & Relaño, M. 2008, ApJ, 675, L17

Gach, J., Hernandez, O., Boulesteix, J., Amram, P., Boissin, O., Carignan, C., Garrido, O., Marcelin, M., Östlin, G., Plana, H., & Rampazzo, R. 2002, PASP, 114, 1043

Hernandez, O., Fathi, K., Carignan, C., Beckman, J., Gach, J., Balard, P., Amram, P., Boulesteix, J., Corradi, R. L. M., de Denus-Baillargeon, M., Epinat, B., Relaño, M., Thibault, S., & Vallée, P. 2008, PASP, 120, 665

Hernandez, O., Gach, J., Carignan, C., & Boulesteix, J. 2003, in Presented at the Society of Photo-Optical Instrumentation Engineers (SPIE) Conference, Vol. 4841, Society of Photo-Optical Instrumentation Engineers (SPIE) Conference Series, ed. M. Iye & A. F. M. Moorwood, 1472–1479

Hernandez, O., Wozniak, H., Carignan, C., Amram, P., Chemin, L., & Daigle, O. 2005, ApJ, 632, 253

Shapiro, K. L., Genzel, R., Förster Schreiber, N. M., Tacconi, L. J., Bouché, N., Cresci, G., Davies, R., Eisenhauer, F., Johansson, P. H., Krajnović, D., Lutz, D., Naab, T., Arimoto, N., Arribas, S., Cimatti, A., Colina, L., Daddi, E., Daigle, O., Erb, D., Hernandez, O., Kong, X., Mignoli, M., Onodera, M., Renzini, A., Shapley, A., & Steidel, C. 2008, ApJ, 682, 231